Pergamon

Int. J. Heat Mass Transfer. Vol. 41, No. 12, pp. 1719–1728, 1998

Printed in Great Britain
0017–9310/98 $19.00+0.00

PII: S0017–9310(97)00280–9

The behavior of a fire-protection foam exposed to radiant heating

CHRISTOPHER F. BOYD
U.S. Nuclear Regulatory Commission, Washington, D.C. 20555, U.S.A.

and

MARINO DI MARZO†
Mechanical Engineering Department, University of Maryland, College Park, MD 20742, U.S.A.

(*Received* 23 *January* 1997 *and in final form* 29 *August* 1997)

Abstract—A one-dimensional, steady-state model is developed which predicts the behavior of a fire-protection foam exposed to radiant heating. Foam evaporation rate, energy balance, and temperature distribution within the foam are calculated for a given radiant heat input and foam expansion ratio. Results indicate that the energy balance is dominated by heat absorption and evaporation. The model is compared to experimental data from foam samples exposed to heat input from gas-fired panels. Measured and calculated temperature profiles are in good agreement. Dimensionless results remove the dependence on heating rate and collapse the temperature gradient in the bulk of the foam layer to a single value. © 1998 Elsevier Science Ltd. All rights reserved.

INTRODUCTION

The protection of structures is a common application for fire-fighting foams. In the presence of fire, structures can be coated with foams which shield the underlying surface from the heat. These foams have good insulation properties and absorb heat, which is dissipated through vaporization. The maximum underlying surface temperature is limited to the evaporation temperature as long as water is present. Foams are a very efficient means of using the available water [1]. California's wildfires have become increasingly costly as more homes are built in areas prone to wildfire. A wildfire typically passes a home in as little as five minutes. This time is shorter than the expected lifetime of a properly applied foam. The structure can be coated in advance of the fire arrival which minimizes the danger to the fire-fighters involved. Foams stick under eaves, in corners, and to window glass which are all suspected areas for fire to enter a home. No structure has been lost to California wildfires when properly coated with foam [2].

Standardized test procedures to assess foams performance have been developed with fire-fighting in mind. However, requirements for a good fire-fighting foam may render it useless in a fire-protection application. A good fire-fighting foam should flow freely to cover pool fire fuel surfaces quickly. In contrast, foam used to protect vertical surfaces must stick in place to maintain a protective barrier. Guidelines for the selection of foams for fire-protection applications need to be developed. Typical literature on foam usage in the fire environment concentrates on the ability of foam to suppress existing fires of various types [3–5]. The use of foams in a fire-protection role is emerging, and tests, specific to fire-protection applications, are limited. No reports have been found which measure or predict the behavior of the foam while it is subjected to radiant heating.

The present research is focussing on foams designed to protect structures exposed to fire. Compressed air foams are typically used for fire-protection applications because of their inherent properties that enable them to stick and cling to vertical and overhanging surfaces. In addition, the water does not drain from these foams at any appreciable rate. The appearance and feel of the foams is similar to shaving or whipped cream.

Literature concerning fire-protection foam testing typically documents the overall effectiveness of a foam used to protect a specific structure or material. Madrzykowski [6] used compressed air foam to coat vertical plywood and subjected the specimens to radiant heating. Time delay to ignition for foamed plywood was twice that for plywood coated with water only. The applied foam thickness was chosen to hold an amount of water equal to the amount used in the water-only tests. The application of more foam would magnify the reported ignition delay times. Perrson [7] looked closer at the overall behavior of the foam during exposure to radiant heating. His tests measured

† Author to whom correspondence should be addressed. Fax: 301-314-9477. E-mail: marino@eng.umd.edu.

NOMENCLATURE

c	specific heat
C	proportionality constant
f	liquid volume fraction
h_v	latent heat of vaporization
i	radiant heat flux
k	thermal conductivity
$\dot{q}_r$	radiative source term
$\dot{q}_e$	evaporative sink term
T	temperature
u	velocity
V	volume
x_p	expansion ratio : ρ_f/ρ_l
z	coordinate in the depth of the foam layer (see Fig. 6).

Greek symbols

δ	characteristic length
ζ	non-dimensional coordinate : z/δ
θ	non-dimensional temperature : $(T-T_0)/(T_i-T_0)$
κ	extinction coefficient
ρ	density
χ	non-dimensional term in equation (14).

Subscripts

a	air component
f	foam component
i	value at the foam exposed interface
l	liquid component
v	vapor component
λ	spectral dependence
0	initial value.

foam drainage and foam evaporation rates for foams subjected to radiant heat fluxes ranging up to 35 kW m^{-2}. Evaporation rates were proportional to the incident radiation level. Drainage rates for the foams increased when subjected to radiant heating. Foam breakdown accelerated by the radiation is the suspected cause. The foams used by Perrson were typical fire-fighting agents with expansion ratios ranging from 6.5–11.5 applied to a horizontal test bed.

The goal of the present study is to identify properties within the foam which govern its overall behavior. A repeatable test is developed to evaluate the destruction of fire-protection foams subjected to radiant heating. A vertical steel plate is covered with foam and placed in front of a set of gas-fired panels. Observations and measurements within the foam during these experiments are used to identify the parameters needed to model the foam evaporation process. Quantitative experimental results are used to guide the model's assumptions and assess its predictive capability. Individual terms of the energy equation are evaluated with separate sets of specific experiments. Relative importance of the governing parameters is obtained from an order of magnitude analysis and from the model results.

EXPERIMENTS

The objective of the experimental study is to determine the behavior of fire-protection foam in the presence of fire. The foam behavior is determined as a set of quantitative measurements of the foam temperature distribution along with qualitative observations of the foam during a specific test. These tests consider foam used to protect vertical structures exposed to fire. Only the effect of heat radiation on the foam is considered. Other effects (i.e. wind, weathering, etc.) which influence a foam's fire-protection capability will be the topic for further studies.

Foam characterization

A custom built compressed air foam generator is used to produce the foam. A schematic representation of the foam generator used for this study is illustrated in Fig. 1. Air pressurizes a 3% concentrate–water foam solution and drives it through a small orifice in a coaxial mixer. A second air stream passes through a needle valve and joins the solution. Exiting the coaxial mixer, the air and solution mixture expand into a

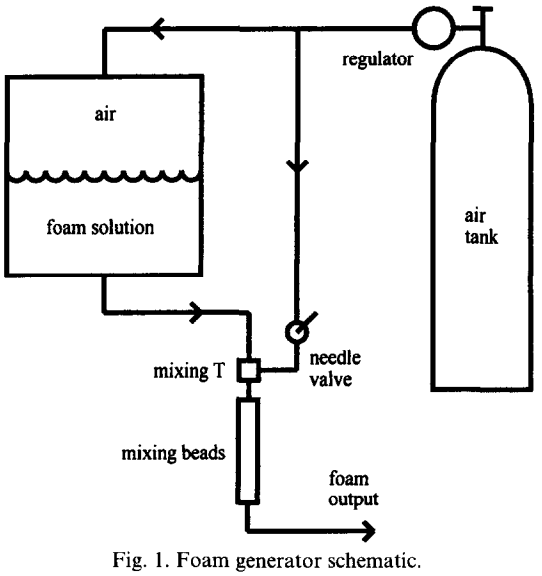

Fig. 1. Foam generator schematic.

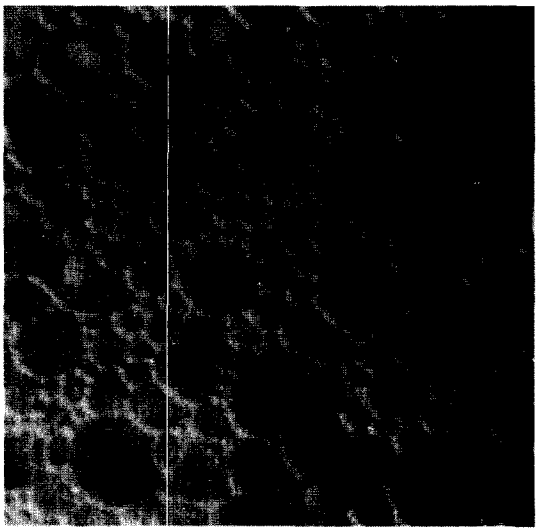

Fig. 2. Typical foam structure ($x_p = 27$).

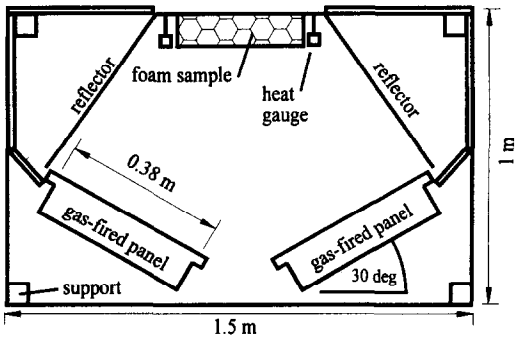

Fig. 3. Foam test apparatus.

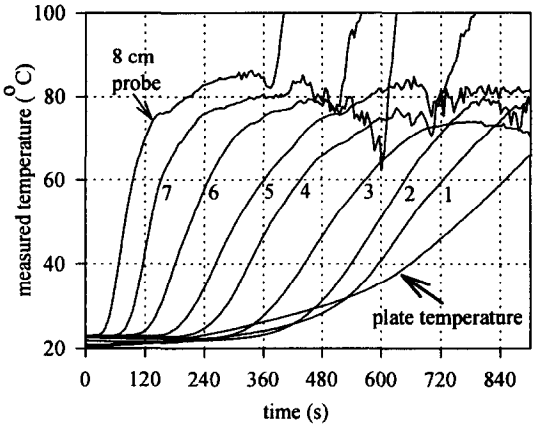

Fig. 4. Temperature transient at various depths in a 0.10 m foam layer deposited on a metal plate ($x_p = 18$; $i_i = 17.5$ kW m^{-2}; distances measured from plate).

packed bed of beads where the air and solution mix to produce foam. Control over the process is obtained by adjusting the air–foam-solution ratio. The expansion ratio is used to characterize the foams. The expansion ratio is defined as the ratio of the volume of foam produced and the volume of foam concentrate used. Foam expansion ratios investigated here are ranging from 12–32.

A commercially available foam, recommended for fire-protection applications [8] is selected for evaluation. Once applied, this foam remains in place for more than 24 h at room conditions. The foam sticks to vertical and inverted surfaces in layers of 0.10 m. The upper limit on foam layer thickness has not been determined. Figure 2 depicts the typical foam structure.

Foam testing apparatus

Two vertical gas-fired panels, 0.38×0.83 m^2, are used to supply the heat input. Within the panels a regulated mixture of natural gas and air can generate heat fluxes up to 18 kW m^{-2} at the foam surface. Figure 3 provides a top-view of the components which make up the foam test apparatus. The panels are oriented at a 30° angle as shown in the figure which helped to produce a uniform radiation field at the foam front. Reflector panels on the sidewalls help maximize the heat applied to the foam. The foam sample is positioned at the center height of the gas-fired panels. Reference heat flux gauges are mounted on each side of the sample to monitor the heat flux level. To verify the heat flux uniformity, reference measurements are made over a three-dimensional array of points covering the volume occupied by the foam. This experimental determination of the uniformity indicates a standard deviation in the heat flux over the test volume of approximately 4% of the applied flux.

Foam samples are applied to a 0.30×0.30 m^2 square steel plate which is instrumented with thermocouples. One thermocouple measures the plate temperature and eight thermocouples measure the foam temperature at distances of 0.01–0.08 m from the plate. The eight thermocouples within the foam are positioned in 45° increments on a 0.04 m circle in the middle of the plate. The plate thermocouple is positioned at the center of this circle.

Test procedure

The test plate is covered with a uniform blanket of foam and tested immediately to minimize any effect of foam aging. The expansion ratio is obtained by weighing one liter of foam and taking the reciprocal of this measurement expressed in kilograms. Note that the density of water is approximately one kilogram per liter. Two samples of the foam, taken immediately before and after covering the plate, exhibit expansion ratios usually within 1% of each other.

Figure 4 illustrates the measured temperature rise for a plate covered with 0.10 m of foam having an expansion ratio of 18 and exposed to 17.5 kW m^{-2} of

heat radiation. Temperature traces are labeled 1–8 indicating distance from the plate surface expressed in centimeters. During this 15 min test, several observations are made:

(a) each thermocouple responds in a similar manner;
(b) temperature remains at its initial value while the foam insulates the thermocouple from the applied heat flux;
(c) the thermocouples respond gradually for a few seconds before rising at a nearly constant rate to approximately 70°C;
(d) once at 70°C, the rate of temperature rise slows and the temperature asymptotically approaches 80°C;
(e) measured temperatures near the end of each trace are erratic and 80°C is chosen as an average value for the front temperature. At some point, each trace jumps over 100°C indicating that the foam front has moved past the thermocouple exposing it to direct radiation from the gas fired panels.

It is assumed that most of the data from Fig. 4 represent steady-state results since several of the temperature traces are similar. A steady-state velocity is obtained by equating the heat applied with the rate of enthalpy change of the material. For the test conditions of Fig. 4, the steady-state ablation velocity is 0.126 mm s^{-1}. Shifting the data to account for the spatial separation of the probes and converting the time axis to a distance axis results in Fig. 5. Traces 0, 1, 7, and 8 are dropped because they are influenced by the plate or by the initial heat-up transient. The traces of Fig. 5 are overlapped suggesting that the steady-state assumption is valid. Differences in the traces are attributed mainly to the non-uniformity of the foam front.

FOAM ABLATION MODEL

The classic solid material ablation problem [9, 10] is used as a starting point for the foam ablation model.

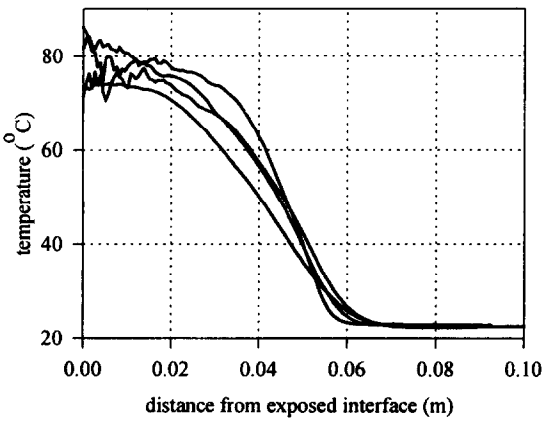

Fig. 5. Temperature traces in a Lagrangian frame which follows the foam exposed surface ($x_p = 18$; $i_i = 17.5$ kW m^{-2}).

In typical ablation solutions, the energy equation is solved in a reference frame moving with the ablation boundary. Incoming heat at the solid surface is: (a) absorbed as heat of ablation; and (b) conducted into the solid material. The ablation velocity is obtained from an energy balance at the surface. The boundary conditions are the melting point temperature and the initial temperature of the material. The solution is a time independent temperature distribution which moves with the foam front.

Foam is not a typical ablative material. The assumptions in the ablation solution are modified to account for the unique properties of foam as noted below:

(a) radiation is absorbed in depth and is accounted for with a volumetric source term;
(b) a variable velocity and density field are needed to account for the foam's expansion;
(c) a volumetric vaporization term is needed to account for the local vaporization of the liquid within the foam;
(d) thermodynamic equilibrium is assumed [11];
(e) saturated conditions are assumed in consideration of the very large specific surface area of the foam cell walls and the relatively long time scale of the foam's destruction process [12];
(f) the liquid is assumed stationary with respect to the foam structure which implies that liquid does not drain from the structure or move through the structure in any way;
(g) air and vapor have the ability to escape from the foam structure;
(h) the velocity of the gases are different from the liquid;
(i) air and water vapor are considered ideal gases and total pressure is 1 atm;
(j) the thin walls of the foam cannot support a significant pressure difference and the effect of surface tension is deemed insignificant.

Model formulation

A steady-state solution approach is used to evaluate the foam ablation problem. As illustrated by Figs. 4 and 5, this approach represents a significant portion of the data available from the foam ablation tests. The basic equations governing the foam ablation model are determined from the fundamental conservation laws. For this problem, momentum conservation is not playing a dominant role. Mass conservation is used to determine the rate of liquid vaporization and the foam component velocities in the convective term of the energy equation. The energy equation which summarizes the steady-state foam ablation model can be written as:

$$\frac{\mathrm{d}}{\mathrm{d}z}\left(k\frac{\mathrm{d}T}{\mathrm{d}z}\right)-\rho_f c u\frac{\mathrm{d}T}{\mathrm{d}z}+\dot{q}_r+\dot{q}_e=0 \qquad (1)$$

where $\dot{q}_r$ and $\dot{q}_e$ are the source and sink terms for

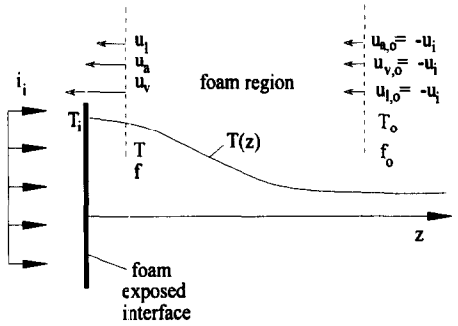

Fig. 6. Coordinate system and convective flows schematics.

radiation absorption and foam evaporation, respectively. The solution to equation (1) requires boundary conditions, property relations, and the mass conservation statements for water, air and vapor which will provide the velocity of these components in the convective term of the energy balance. Figure 6 depicts the coordinate system for equation (1) which moves with the foam front with the z-axis directed into the depth of the foam. The boundary conditions are T_i (i.e. the exposed interfacial temperature which is determined experimentally), at the foam front (at $z = 0$), and T_0 (i.e. the initial ambient conditions temperature), at the initial foam temperature for large values of z.

SUB-MODELS

In order to solve the foam ablation model outlined above, models for the individual terms are developed. Where necessary, terms are developed based upon sets of specific experiments.

Radiative source term

The radiative source term accounts for the absorption of thermal radiation. No data are readily available on a fire-protection foam absorption characteristics so experimental results along with simplifying assumptions are used to estimate the radiation absorption characteristics. It is assumed that all incoming radiation is absorbed by the foam. The radiation attenuation in the depth of an absorbing and scattering material is given by the Bouguer's Law which gives a relation for the intensity as a function of penetration distance z:

$$i_\lambda = i_{i,\lambda} e^{-\int_0^z \kappa_\lambda dz}. \tag{2}$$

The constant, κ_λ, is the extinction coefficient. The extinction coefficient measures how fast the radiation is diminished through absorption and scattering and, in general, increases with density. The extinction coefficient is the summation of the absorption coefficient and of the scattering coefficient [13]. The subscript λ indicates the spectral dependence of these properties. If one assumes the properties are independent of wavelength, it is possible to obtain an estimate for the extinction coefficient from relatively simple experiments. In the foam ablation model, the foam and radiation source are one-dimensional and the net scattering is zero. However, the experimental setup for the measurements of the extinction coefficient is not one-dimensional. Therefore, scattering plays a significant role and a method for evaluating the scattering coefficient is proposed.

A heat flux gauge, sensitive to radiation in the infrared, is used as the detector. The data for several different foam samples are collected and indicate that the extinction coefficient rises with an increase in foam density as expected. The effect of scattering is determined by minimizing the effect of absorption. Water is a strong absorber of heat radiation in the infrared region, but is effectively transparent to radiation with wavelengths less than 1 μm. Using a photodetector sensor, which is only sensitive to wavelengths smaller than 1 μm, extinction coefficients are determined which represent a good estimate for the scattering coefficient. The scattering coefficient is assumed to be wavelength independent since the scattering is principally governed by geometric optics [14]. Results indicate that the scattering coefficient is independent of foam density over the range of densities tested. The one-dimensional extinction coefficient (to be used in the foam model) is obtained using the measured values for the extinction deducted of the measured scattering coefficient. Since one can assume no radiation absorption for a zero density medium, this condition is imposed by using a proportionality functional to fit the data (i.e. $\kappa = C\rho$). From these experiments, the proportionality constant, C, is found to be 3 $m^2\,kg^{-1}$. The radiative source term in equation (1) is the spatial derivative of the intensity function and can be obtained as:

$$\dot{q}_r = -\frac{d}{dz}(i_i e^{-\int_0^z \kappa dz}). \tag{3}$$

Foam density

Evaluation of equation (3) requires knowledge of the density distribution since κ is a function of ρ_f. The problem of specifying a density function for the foam lies in the dynamic nature of the foam material: (a) foam is constantly changing; (b) liquid evaporates from the foam; (c) bubbles burst and coalesce with one another; and (d) air and vapor escape from the foam. All of these processes change the density of the foam and take place at different rates depending upon the surrounding conditions. An exhaustive foam density model is at least a function of temperature, humidity, foam structure breakdown rates, and time. A simplified approach to determining a density function is proposed in order to obtain a solution to the foam ablation problem.

The foam density is related to the individual component densities by the liquid volume fraction (f) as:

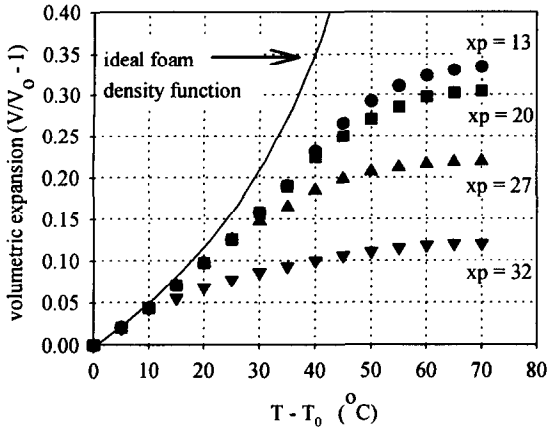

Fig. 7. Foam volumetric expansion as a function of temperature rise for various initial foam expansion ratios.

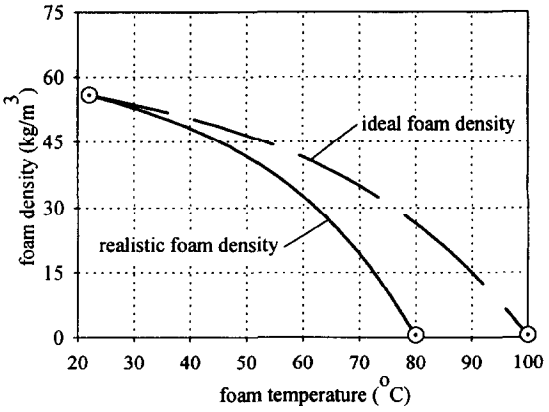

Fig. 8. Foam density functions: ideal foam model vs. postulated realistic model.

$$\rho_f = \rho_l f + (\rho_v + \rho_a)(1-f). \tag{4}$$

The initial density is obtained from mass and volume measurements. Foam expansion measurements give quantitative data on the foam's expansion characteristics. A beaker containing a volume of foam, V_0, at a uniform initial temperature is placed in a convection oven at a fixed temperature. The volume of the foam, V, is recorded when the foam temperature reaches the oven temperature. Foam expansion is defined as V/V_0. Figure 7 illustrates the curve fit data obtained from these experiments for expansion ratios of 13, 20, 27, and 32. The data indicate that the higher-expansion-ratio, dry foam, is unable to expand as far as the wetter, low-expansion-ratio foam. Bubbles in the high-expansion-ratio foam tended to burst at lower temperatures letting air and vapor escape.

The upper curve on the plot (i.e. the solid line) represents the behavior of the ideal foam. The ideal foam model evaluates the volumetric expansion from the perfect gas law written for the air and steam trapped in the foam. The amount of steam is calculated from the equilibrium conditions at the foam temperature. This model serves as a theoretical upper bound of the foam's expansion where neither air nor steam are allowed to escape from the foam matrix.

A foam density function is obtained by transforming the ideal foam density function such that the model agrees with the physical measurements and observations. First, it is observed that the foam does not break down very rapidly at low temperatures. Next, it is observed that the foam temperatures level out at approximately 80°C during foam ablation tests. Figure 8 illustrates the foam density function along with the ideal foam density model (i.e. no-gas escaping from the foam). The foam density function is obtained by linearly transforming the temperature scale from the ideal density function. The end-point at 80°C is determined from experimental observations. The density function has the required characteristics and it is considered to be a reasonable estimate of the foam density as a function of temperature for the purposes of deriving the steady-state foam ablation model.

Velocities

A steady-state–steady-flow control volume analysis is used to compute the ablation velocity. The control volume moves with the foam front at the ablation velocity as shown in Fig. 6. The ablation velocity is determined by equating the incoming radiant energy to the rate of enthalpy change of the foam components as they pass through the control volume. As the foam expands, air and vapor escape. The velocity of each component is quantified using conservation of mass. The liquid is assumed stationary with respect to the foam structure. The liquid velocity is related to the foam front velocity by considering the foam expansion V/V_0. Therefore, one can write:

$$u_l = -V/V_0 u_i. \tag{5}$$

The relation for air velocity is given by:

$$u_a = -\frac{(1-f_0)\rho_{a,o}}{(1-f)\rho_a} u_i. \tag{6}$$

The vapor velocity is obtained from:

$$u_v = \frac{-\rho_l f_0 u_i - \rho_l f u_l}{\rho_v (1-f)} = -\frac{\rho_l f_0 - \rho_l f V/V_0}{(1-f)\rho_v} u_i. \tag{7}$$

With these component velocities, the convective term of equation (1) can be written as:

$$\rho_f c u = -\rho_l f_0 u_i c_l \left[\frac{fV}{f_0 V_0} + \left(1 - \frac{fV}{f_0 V_0}\right)\frac{c_v}{c_l} + \frac{\rho_{a,o}}{\rho_l}\frac{1-f_0}{f_0}\frac{c_a}{c_l}\right]. \tag{8}$$

The term in square brackets is non-dimensional and will be identified in the following as χ.

Evaporative sink term

The evaporative sink term of the energy conservation statement accounts for the energy absorbed as liquid is vaporized. The liquid vaporization rate is obtained from liquid continuity and is multiplied by the heat of vaporization to obtain:

$$\dot{q}_e = \rho_l h_v \frac{d}{dz}(f u_l) = -\rho_l f_0 u_i h_v \frac{d}{dz}\left(\frac{fV}{f_0 V_0}\right). \quad (9)$$

Thermal conductivity

It will be shown that the thermal diffusion plays a minor role in the energy balance for the foam ablation model. Therefore, the thermal conductivity is assumed constant. A transient measurement technique outlined by Kennedy [15] is used to approximate the thermal conductivity of the fire-protection foam. The thermal conductivity is determined to be 0.1 W mK^{-1}. This result is close to the predictions by the thermal conductivity model of Glicksman and Torpey [16] which is derived for closed-cell foams with a nominal bubble diameter of 300 μm which is consistent with the foam structure characteristics shown in Fig. 2.

Non-dimensional governing equation

Let us introduce the non-dimensional temperature θ which references the temperature to its initial value and to the foam exposed interfacial value previously discussed. The characteristic length is selected considering the radiative source term. The extinction coefficient for the foam in its initial state is given as:

$$\kappa_0 = 3\rho_{f,o} = 3\rho_l \frac{\rho_{f,o}}{\rho_l} = 3\frac{\rho_l}{x_p}. \quad (10, 11, 12)$$

From here, a characteristic length is introduced as $\delta = 1/\kappa_0$ which is an explicit functional of the foam expansion ratio and relates to the radiation penetration length. Therefore, the non-dimensional coordinate is $\zeta = z/\delta$. The energy balance described in equation (1) is written in non-dimensional terms using these definitions and the submodels previously described. By normalizing the terms of the non-dimensional equation with respect to the coefficient of the forcing function (i.e. the radiative source term), one obtains:

$$\left[\frac{k_f(T_i - T_0)/\delta}{i_i}\right]\frac{d^2\theta}{d\zeta^2} - \left[\frac{\rho_l f_0 u_i c_l (T_i - T_0)}{i_i}\right]\chi\frac{d\theta}{d\zeta} - \frac{d}{d\zeta}e^{-\int_0^\zeta \frac{\kappa}{\kappa_0}d\zeta} - \left[\frac{\rho_l f_0 u_i h_v}{i_i}\right]\frac{d}{d\zeta}\left(\frac{f}{f_0}\frac{V}{V_0}\right) = 0. \quad (13)$$

The non-dimensional coefficients preceding the various terms represent heat fluxes referenced to the radiant heat flux at the foam exposed interface. Table 1 summarizes the significance of each coefficient and provides a relative order of magnitude. From these estimates, conduction and convection are expected to be of secondary importance to the radiative and evaporative heat fluxes.

NUMERICAL SOLUTION

A numerical procedure is used to solve the foam ablation model. The steady-state solution is approached asymptotically using a second-order Crank–Nicholson technique to advance the solution. The radiative source term is fixed during the solution of equation (13), thus an iterative solution is necessary. The boundary conditions are obtained from the foam test conditions. The foam front temperature is set to 80°C based on experimental observations. The far-field temperature is set to the initial temperature of the foam. The solution of equation (13) for the conditions of the data depicted in Fig. 5 is illustrated in Fig. 9. The numerical and experimental results display the same behavior.

The terms in equation (13) are computed individually to compare the relative importance of each term in the energy balance. Figure 10 illustrates the terms in the energy balance as a function of the distance from the foam front. The radiative source and evaporative sink terms represent the largest contributors to the energy balance and are approximately mirror images of one another. Note that the radiation absorption is low at the foam surface because the density of the medium is low in that region. Radiation

Table 1. Non-dimensional coefficients

Coefficient	Significance	Order of magnitude
$\frac{k_f(T_i - T_0)/\delta}{i_i}$	Heat flux by conduction referenced to the radiant heat flux at the foam exposed interface	~0.07 One order of magnitude less than the driving term
$\frac{\rho_l f_0 u_i c_l (T_i - T_0)}{i_i}$	Heat flux by convection referenced to the radiant heat flux at the foam exposed interface	~0.08 One order of magnitude less than the driving term
$\frac{\rho_l f_0 u_i h_c}{i_i}$	Heat flux by evaporation referenced to the radiant heat flux at the foam exposed interface	~0.5 Same order of magnitude of the driving term

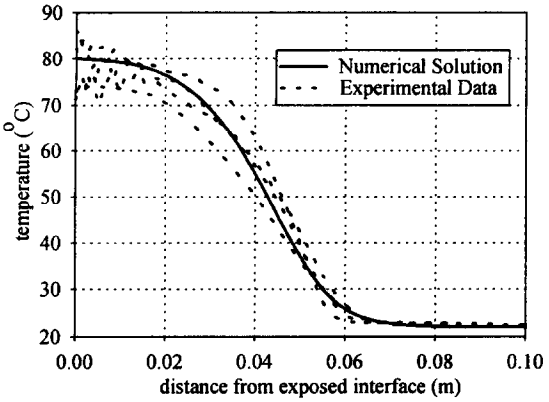

Fig. 9. Comparison of model results with measured temperature traces ($x_p = 18$; $i_i = 17.5$ kW m^{-2}).

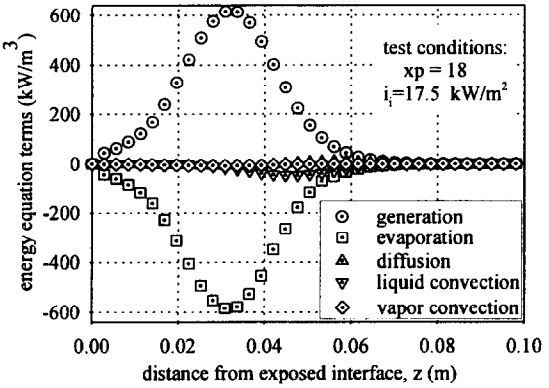

Fig. 10. Relative contribution of the energy balance terms in the depth of the foam layer ($x_p = 18$; $i_i = 17.5$ kW m^{-2}).

absorption peaks at about 0.03 m from the foam front. This is due to the contribution of the radiation attenuation and the increasing absorption due to the increasing density of the medium. The anti-symmetrical behavior of the radiative source and vaporization terms indicates that energy deposited by radiation is used to vaporize liquid at the point of absorption.

The next largest term, the liquid convection, is less than 10% of the magnitude of the radiative source term. Vapor convection as well as thermal diffusion play only minor roles in the energy balance. The energy associated with the air convection term is negligible and is not shown in the figure.

RESULTS AND DISCUSSION

Foam testing

A total of 26 foam tests with various foam expansion ratio and applied heat flux combinations are performed. Heat flux ranged from 10–18 kW m^{-2} and expansion ratio varied from 13–33. Three of the 26 tests are eliminated because the data did not reach steady state conditions. These sets consisted of the lowest heat flux, lower expansion ratio cases. In eight tests, significant portions of the foam fell from the plate during the test. These events caused these tests to be dropped from consideration. The remaining 15 data sets are used for comparison with the foam ablation model.

All experimental data are transformed into an equivalent steady state temperature profile as described earlier. For comparison, each profile is broken down into three regions. The profiles are flat near the foam front and decrease gradually from 80°C to about 70°C. From 70°C the profiles further decrease at a nearly uniform rate until they reach about 35°C. From this point, the temperature gradient asymptotically approaches the unheated foam temperature. The experimental results are quantified based on the average temperature gradient between 35 and 70°C (i.e., in the core of the foam). Four traces make up each data set so an average and a standard deviation are computed. Comparisons based on the end regions of the temperature profile are not attempted due to the irregularities of the experimental data in these regions.

The average temperature gradient is found not to be a function of the applied heat flux for the given data set. However, the gradient is a function of the foam expansion ratio as illustrated by Fig. 11. Results from the foam ablation model are also plotted and indicate that the gradient decreases as the foam expansion ratio increases. The model results lie within one standard deviation of all but five data points. Two main reasons account for an upward bias observed in the data: (a) small sections of foam falling from plate; (b) failure to reach steady state conditions. Both of these phenomena will result in larger values of the temperature gradient.

Based on the ability of the numerical model to predict the experimental results, it is assumed that the model accounts for the major phenomena which govern the foam ablation process.

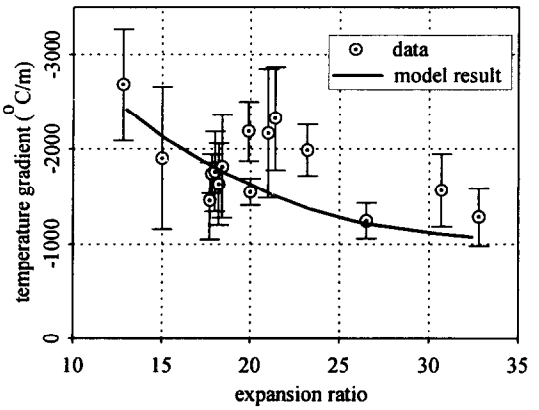

Fig. 11. Temperature gradient in the bulk of the foam layer; model predictions vs data (x_p from 13–33; i_i from 17–18 kW m^{-2}).

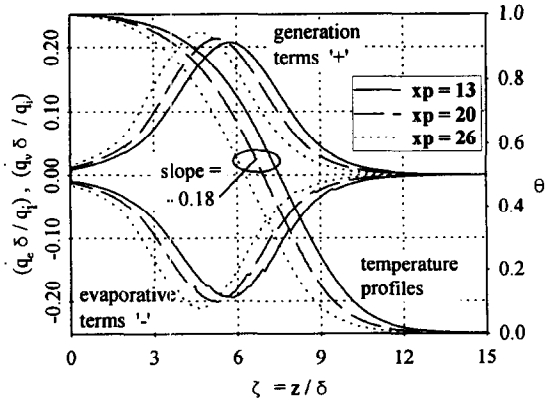

Fig. 12. Summary of model predictions in dimensionless form.

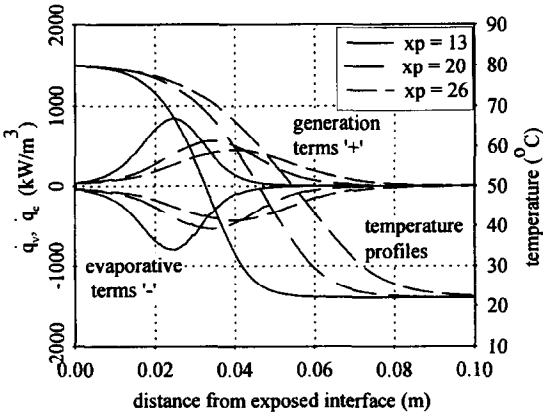

Fig. 14. Effect of foam expansion ratios: model predictions at $i_i = 17.5$ kW m^{-2}; x_p from 13–26.

Model results

In dimensionless form, the results of the model are summarized in Fig. 12. The temperature profiles take on a more consistent shape. The profiles differ only in the end regions. The average dimensionless temperature gradient in the central region of the curves collapses to a single value of -0.18. This value is a universal result of this model and holds for all expansion ratios and sufficiently high heat fluxes.

The average experimental temperature gradient in dimensionless form is -0.21 ± 0.04. This value is 17% greater than the model result. The numerical prediction of -0.18 lies within one standard deviation of the experimental result. The model result predicts a temperature gradient which is smaller in magnitude than the average experimental value. Reasons which bias the experimental values to larger magnitudes have been outlined earlier. The radiative source and evaporation terms are almost mirror images of one another. This reinforces the fact that energy is absorbed by the foam and used almost entirely to evaporate liquid at the point of absorption.

Three calculations are summarized in Fig. 13 for a foam expansion ratio of 18 and heating rates of 10, 20, and 30 kW m^{-2}. The initial and foam front temperature of 22 and 80°C were used for each. The temperature profiles show very little difference. The radiative source and evaporative terms are proportional to the applied heat flux. This can be seen from the governing equations. In fact, each of the terms in the foam model are proportional to the applied heat flux with the exception of the diffusion term. At the lower heating rates, the role of diffusion increases as illustrated in Table 1.

Three calculations are summarized in Fig. 14 for an applied heat flux of 17.5 kW m^{-2} and foam expansion ratios of 13, 20 and 26. The temperature profiles penetrate farther into the foam as the expansion ratio increases. This is explained by the lower average absorption coefficient for the higher expansion ratio foam. The radiative source and evaporative sink terms are still mirror images of each other but vary substantially with expansion ratio. The wetter low expansion ratio foam absorbs the radiation over a shorter distance which results in a relatively large term.

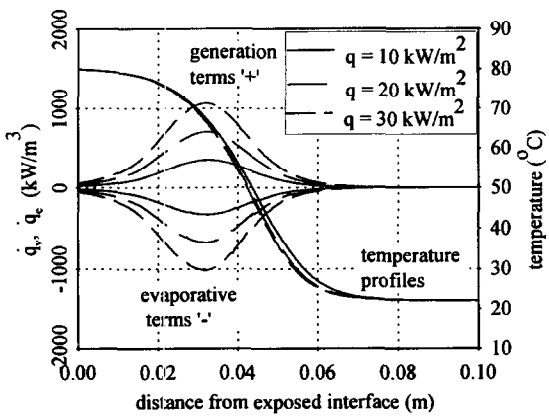

Fig. 13. Effect of incident radiant fluxes: model predictions at ($x_p = 18$; i_i from 10–30 kW m^{-2}).

CONCLUSIONS

The data show that the evaporation of fire-protection foam exposed to flame radiation can be described as steady-state for a major portion of the process. The velocity of the foam front, as the foam evaporates away, is proportional to the applied heat flux. Radiation penetrates the foam several centimeters before being completely absorbed. As the foam expands when heated, the liquid structure breaks down and lets air and vapor escape. The proposed model accurately predicts the steady-state temperature profile within the fire-protection foam exposed to radiation. The radiation absorption and liquid vaporization terms dominate the solution. Radiation absorbed by the foam is mainly used to evaporate liquid at the point of absorption.

Acknowledgements—This research was funded by the Building and Fire Research Laboratory at the National Institute of Standards and Technology. The encouragement and support of Drs D. Evans and H. Baum is greatly appreciated.

REFERENCES

1. Colletti, D. J., Quantifying the effects of class A foam in fire fighting. *Fire Engineering*, 1993, **146**(2), 41–44.
2. Rochna, R. R., Foam on the range. *Fire Chief*, 1994, **38**(6), 34–38.
3. Briggs, A. A. and Webb, J. S., Gasoline fires and foams. *Fire Technology*, 1988, **24**(1), 45–58.
4. Wesson, H. R., Welker, J. and Brown, L., Control LNG-spill fires. *Hydrocarbon Processing*, 1972, **51**(12), 61–64.
5. Stechishen, E., *The Effectiveness of Forest Fire-Fighting Foams*. Petawawa National Forestry Institute Technical Report, Ontario, Canada, 1991.
6. Madrzykowski, D., *Study of the Ignition Inhibiting Properties of Compressed Air Foam*. National Institute of Standards and Technology, NISTIR 88-3880, Gaithersburg, MD, 1988.
7. Perrson, H., Fire extinguishing foams resistance against heat radiation. *Proceedings, 1st International Conference on Fire Suppression Research*. Swedish National Testing and Research Institute, Stockholm, 1992, pp. 359–376.
8. Biddle, S., Chubb National Foam Representative, personal communication concerning applicability of Durra Foam product for fire-protection applications, June 1994.
9. Carslaw, H. S. and Jaeger, J. C., *Conduction of Heat in Solids*. Clarendon Press, Oxford, 1959.
10. Rohsenow, W. M. and Choi, H., *Heat, Mass, and Momentum Transfer*. Prentice-Hall, Englewood Cliffs, 1961, pp. 122–124.
11. Morrison, F. A. Jr., Transient multiphase multicomponent flow in porous media. *International Journal of Heat and Mass Transfer*, 1973, **16**, 2331–2342.
12. Sahota, M. S. and Pagni, P. J., Heat and mass transfer in porous media subject to fires. *International Journal of Heat and Mass Transfer*, 1979, **22**, 1069–1081.
13. Siegel, R. and Howell, J. R., *Thermal Radiation Heat Transfer*. Hemisphere Publishing Company, U.S.A., 1981.
14. Howell, J. R., Baker–Hughes Centennial Professor, University of Texas at Austin, personal communication concerning absorption and scattering coefficients, 1995.
15. Kennedy, W. L., *An IBM Computer Program for Determining the Thermal Diffusivity of Finite Length Samples*. USAEC IS-137, 1960.
16. Glicksmann, L. R. and Torpey, M. R., *A Study of Radiative Heat Transfer Through Foam Insulation*. ORNL/Sub/86-09099/3, 1988.